Regulation of Force Development Studied by Photolysis of Caged ADP in Rabbit Skinned Psoas Fibers

Zhe Lu, Darl R. Swartz, Joseph M. Metzger, Richard L. Moss, and Jeffery W. Walker
Department of Physiology, University of Wisconsin, Madison, Wisconsin 53706 USA

ABSTRACT The present study examined the effects of Ca^{2+} and strongly bound cross-bridges on tension development induced by changes in the concentration of MgADP. Addition of MgADP to the bath increased isometric tension over a wide range of [Ca^{2+}] in skinned fibers from rabbit psoas muscle. Tension-pCa (pCa is $-\log$ [Ca^{2+}]) relationships and stiffness measurements indicated that MgADP increased mean force per cross-bridge at maximal Ca^{2+} and increased recruitment of cross-bridges at submaximal Ca^{2+}. Photolysis of caged ADP to cause a 0.5 mM MgADP jump initiated an increase in isometric tension under all conditions examined, even at pCa 6.4 where there was no active tension before ADP release. Tension increased monophasically with an observed rate constant, k_{ADP}, which was similar in rate and Ca^{2+} sensitivity to the rate constant of tension re-development, k_{tr}, measured in the same fibers by a release-re-stretch protocol. The amplitude of the caged ADP tension transient had a bell-shaped dependence on Ca^{2+}, reaching a maximum at intermediate Ca^{2+} (pCa 6). The role of strong binding cross-bridges in the ADP response was tested by treatment of fibers with a strong binding derivative of myosin subfragment 1 (NEM-S1). In the presence of NEM-S1, the rate and amplitude of the caged ADP response were no longer sensitive to variations in the level of activator Ca^{2+}. The results are consistent with a model in which ADP-bound cross-bridges cooperatively activate the thin filament regulatory system at submaximal Ca^{2+}. This cooperative interaction influences both the magnitude and kinetics of force generation in skeletal muscle.

INTRODUCTION

Regulation of muscle contraction is a relatively complex process that is initiated by binding of Ca^{2+} to specific low-affinity sites on the thin filament protein troponin (Gordon et al., 2000). A long-standing hypothesis is that Ca^{2+} relieves steric inhibition of myosin binding to actin, presumably by inducing a change in position of tropomyosin within the thin filament (Haselgrove, 1973; Huxley, 1973; Parry and Squire, 1973). This hypothesis was supported by the observation that in the presence of ATP(γS) fibers exhibit Ca^{2+}-regulated stiffness but do not develop tension (Dantzig et al., 1988). Also, the extent of binding of myosin subfragment 1 (S1) to myofibrils has been shown to increase in the presence of Ca^{2+} (Swartz et al., 1990, 1996).

An alternative model of regulation proposes that Ca^{2+} regulates a kinetic transition in the cross-bridge cycle, e.g., the P_i release step (Chalovich et al., 1981; Chalovich and Eisenberg, 1982; Rosenfeld and Taylor, 1987). This model was proposed on the basis of observations that Ca^{2+} regulates acto-myosin ATPase activity but does not significantly influence the binding of myosin S1 to actin (Chalovich et al., 1981; Chalovich and Eisenberg, 1982; Rosenfeld and Taylor, 1987). As evidence for regulation of kinetic transitions in muscle fibers, the rate of tension redevelopment (k_{tr}) following a period of unloaded shortening increased up to 10-fold over the physiological range of Ca^{2+} (Brenner, 1988; Metzger et al., 1989). Rates of tension development following photolysis of caged Ca^{2+} (k_{Ca}) were similarly accelerated as Ca^{2+} concentration was increased (Ashley et al., 1991; Araujo and Walker, 1994, 1996).

There is now considerable evidence that strong binding of myosin S1 (i.e., binding that in intact fibers would result in force generation) can also activate the thin filament (see Gordon et al., 2000, for a review). For example, there is cooperative binding of S1 to regulated actin in solution and activation of myosin ATPase by S1 even in the absence of Ca^{2+} (Bremel and Weber, 1972; Greene and Eisenberg, 1980). In skinned fibers, rigor cross-bridges activate the thin filament to allow interaction of cycling cross-bridges (White, 1970; Moss, 1999; Brandt et al., 1990). Cross-bridges with ADP bound are particularly effective in cooperative activation of the thin filament (Thirlwell et al., 1994). Under the more physiological conditions of 5 mM MgATP, addition of a strong binding S1 analog to skinned fibers dramatically altered the Ca^{2+} dependence of tension development kinetics (k_{tr}) (Swartz and Moss, 1992) suggesting that cross-bridge binding plays a major role in regulation of kinetic transitions. The goal of the present study was to further investigate the relative contributions of Ca^{2+} and cross-bridges to the process of thin filament activation during active tension development. In previous work, we examined the kinetics of tension development following photolysis of caged ADP in skinned skeletal fibers (Lu et al., 1993). We concluded that MgADP binds rapidly to nucleotide-free cross-bridges causing inhibition of ATP binding, inhibition of cross-bridge detachment, and accumulation of cross-bridges in force-generating states (Lu et al., 1993). Here we investigated the effects on tension due to a similar rapid elevation of MgADP at submaximal Ca^{2+}.

Received for publication 25 January 2001 and in final form 3 April 2001.
Address reprint requests to Dr. Jeffery W. Walker, University of Wisconsin School of Medicine, Department of Physiology, 1300 University Avenue, Madison, WI 53706. Tel.: 608-262-6941; Fax: 608-265-5512; E-mail: jwalker@physiology.wisc.edu.

0006-3495/01/07/334/11 $2.00

The results are consistent with a similar competition between MgADP and MgATP for binding to cross-bridges, but in addition, MgADP-bound cross-bridges cooperatively activate the thin filament. The rate of the ensuing tension development process varied markedly with Ca^{2+} concentration, but Ca^{2+} dependence was eliminated by addition of *N*-ethylmaleimide-modified S1 (Nagashima and Asakura, 1982; Williams et al., 1988; Swartz and Moss, 1992) which permitted the number of strongly bound cross-bridges to be varied independent of Ca^{2+} concentration. These results support a mechanism in which strongly bound cross-bridges cooperatively activate the thin filament regulatory system thereby affecting both the number and attachment rate of force-generating cross-bridges.

MATERIALS AND METHODS

Muscle preparation

Single skinned fibers from psoas muscle of male New Zealand rabbits (2.5–3.5 kg body weight) were obtained as described previously (Lu et al., 1993). Fiber segments 2.0–2.5 mm in length were tied to stainless steel troughs with surgical monofilament (Moss et al., 1985). Sarcomere length was adjusted to 2.5–2.6 μm and measured by photography. The physiological apparatus for carrying out isometric force measurements in conjunction with pulse photolysis has been described (Walker et al., 1992). Measurements of k_{tr} at the end of each caged ADP transient were carried out as previously reported (Metzger et al., 1989). The rate constants obtained were not dependent upon the speed of release or re-stretch, the extent of release, or on the duration of the shortening phase.

Stiffness ($\Delta F/\Delta SL$) was determined by applying a sinusoidal length change (<0.1% L_o, 3.3 kHz) to the end of the fiber and then measuring changes in force (F) and sarcomere length (SL) as previously described (Metzger et al., 1989). Force was measured using a Cambridge model 407 force transducer with a resonant frequency of 5 kHz and a step response of 0.1 ms. Sarcomere length was monitored with a resolution of 0.5–1.0 nm/half-sarcomere using the first-order line of a laser diffraction pattern (Metzger et al., 1989).

Solutions

Caged ADP (P^2-1(2-nitrophenyl)ethyladenosine 5′-diphosphate) was synthesized according to the method of Walker et al. (1988), and purified by DEAE-cellulose chromatography using a linear gradient of 0–0.5 M triethylammonium bicarbonate. Contamination of caged ADP by free ADP was less than 1 mol % as judged by analytical HPLC. The efficiency of caged ADP photolysis was 25 ± 3% per flash determined as previously described (Lu et al., 1993).

Activating solutions had the following composition (in mM): 5 ATP (4 MgATP), 9 creatine phosphate, 5.6 $MgCl_2$ (1 free Mg^{2+}), 12 EGTA, 100 *N*-tris[hydroxymethyl]methyl-2-aminoethanesulfonic acid (TES), and sufficient KCl to obtain a final ionic strength of 180 mM. Solution pH was adjusted to 7.00 with KOH. pCa 4.5 solution contained 12 mM $CaCl_2$ and 40 mM KCl, and pCa 9 solution contained no added $CaCl_2$ and 66 mM KCl. Intermediate pCa values were obtained by mixing pCa 4.5 and pCa 9 solutions to the appropriate total Ca^{2+} determined by a computer program that accounts for Ca^{2+}, Mg^{2+}, K^+, Na^+, and H^+ binding to all constituents in the solution (Fabiato, 1988). Stability constants for metal and proton binding to creatine phosphate, phosphate, ADP, ATP, and EGTA were taken from Fabiato (1988). The apparent stability constant for Ca-EGTA after correction for temperature (15°C), ionic strength, and pH was 2.39×10^6 M^{-1}.

Photolysis solutions had the same composition as activating solutions except they contained caged ADP and 1.2 mM free Mg^{2+} before photolysis. No creatine phosphokinase was added. The final concentration of MgADP achieved following photolysis was calculated from the free Mg^{2+} concentration, the concentration of photo-generated ADP, and a MgADP stability constant of 6.24×10^2 M^{-1}. Caged ADP was assumed to bind Ca^{2+} and Mg^{2+} with the same stability constants as for caged ATP, 3.3×10^2 M^{-1} (Walker et al., 1988). Even though caged ADP photolysis efficiency was 25% per flash, only a fraction of the free ADP produced binds to Mg^{2+}. Thus, for photogeneration of 0.10 mM and 0.50 mM MgADP, the required concentrations of caged ADP were 1.0 mM and 5.2 mM, respectively. To maintain an ionic strength of 180 mM, contributions to ionic strength from caged ADP ($2M^+$, A^{2-}; Mg-caged ADP has no net charge), glutathione (M^+, A^-), and in some experiments P_i ($\sim 1.5M^+$, $A^{1.5-}$) were taken into account; 10 mM glutathione was included to protect cellular proteins from photolysis by-products.

Data analysis and modeling

Data collection and analysis have been described previously (Walker et al., 1992; Lu et al., 1993). Two methods were used to analyze tension-pCa relationships. For method 1, data obtained from five to seven fibers were averaged, and the averaged data points were fit to the Hill equation: $P/P_o = n_H(pCa_{50} - p_{Ca})/(1 + n_H(pCa_{50} - pCa))$, where n_H is the Hill coefficient and pCa_{50} is the pCa value ($pCa = -\log[Ca^{2+}]$) at which tension is one-half of its maximal value. For method 2, data for each fiber were fit to the same Hill equation to obtain pCa_{50} and n_H, and these parameters were averaged to obtain mean ± SEM. These alternate methods gave pCa_{50} values that were within 2% of each other and n_H values within 15% of each other. Because simple Hill plots did not always fit the data well (e.g., see Figs. 1 and 5 *A*) double Hill plot transformations (Moss et al., 1983) were also employed giving rise to two Hill coefficients, designated n_{H1} and n_{H2}. Values for n_{H1} and n_{H2} obtained from individual fibers were not considered reliable because of a paucity of data points and a high degree of variability, so only those values obtained from averaged data are given in legends to Figs. 1 and 5 *A*. Tension transients were fit to single-exponential functions using Marquardt's nonlinear regression algorithm and the following equation: $P_t = a + P_0(1 - \exp(-kt))$, where P_t is tension at time t and P_0 is tension at $t = 0$, a is tension before photolysis, k is the first-order rate constant k_{ADP} or k_{tr}. Unless otherwise noted, the single-exponential equation was most appropriate because it gave a smaller standard error of the estimate of k and a smaller variance inflation factor (Glantz and Slinker, 1990) compared with a double-exponential equation or a single exponential with sloping baseline. Modeling of the kinetic scheme in Fig. 7 was accomplished by numerical solution of four differential equations using a modified Runge-Kutta algorithm in the commercial software Mathematica.

Preparation and use of NEM-S1

Myosin and the chymotryptic subfragment of myosin (S1) were purified at 4°C as described previously (Swartz et al., 1990; Swartz and Moss, 1992). S1 was modified with *N*-ethylmaleimide (NEM; Sigma Chemical Co., St. Louis, MO) as described previously (Swartz and Moss, 1992). The reaction was quenched with 1 mM dithiothreitol (DTT), and then the protein was precipitated with ammonium sulfate and stored as a pellet at −20°C. Before use, NEM-S1 was dialyzed against 20 mM imidazole, pH 7.0, 1 mM DTT and then filtered through a 0.45-μm filter. Protein concentration was determined by absorbance at 280 nm using a mass absorptivity value of 0.75 $(mg/ml)^{-1}$ cm^{-1} and a molecular weight of 118,000. Solutions of NEM-S1 were prepared just before use by mixing equal volumes of protein solution and a 2X stock of pCa 9 solution. Skinned fibers were treated with NEM-S1 by incubation in relaxing solution for 20 min and were then transferred to activating solutions without NEM-S1. After each tension

measurement during which the fiber was activated for less than 15 s, the fiber was transferred back into the relaxing solution containing NEM-S1.

RESULTS

Effects of MgADP on steady-state tension and stiffness

As illustrated in Fig. 1, inclusion of MgADP in activating solutions increased maximal tension, shifted the tension-pCa relationship to lower Ca^{2+} concentrations, and tended to increase the Hill coefficient. Changes in tension, pCa_{50}, and n_H were larger at 5 mM MgADP than at 0.5 mM MgADP and in fact were statistically significant only at the higher MgADP level ($p < 0.05$). Stiffness measurements yielded different results. In solutions with no added MgADP, mean stiffness at pCa 4.5 was 49.9 ± 5.3 N/m ($n = 5$), which yielded an elastic modulus of 2.50×10^7 N/m^2 when fiber length and cross-sectional area were taken into account. Stiffness increased slightly (3%) to a mean value of 51.4 ± 3.1 N/m ($n = 5$) in the presence of 5 mM MgADP (Fig. 1, *inset*), but this change was not statistically significant. In contrast, maximum tension increased by 19% (Fig. 1), and as stated above, this was a significant increase. Therefore, this increase in force at pCa 4.5 is not associated with a statistically significant increase in number of strongly attached cross-bridges but instead reflects an increase in force per cross-bridge. Sarcomere stiffness at pCa 6.1 was normalized to that measured at pCa 4.5 with the same concentration of MgADP. This relative stiffness at pCa 6.1 increased from a mean value of 0.57 ± 0.06 in the absence of MgADP to 0.74 ± 0.05 in the presence of 5 mM MgADP (Fig. 1, *inset*). This represents a 29% increase in sarcomere stiffness due to MgADP. For comparison, steady-state tension at pCa 6.1 increased from 0.33 ± 0.02 to 0.53 ± 0.02, a 61% increase. Paired *t*-tests indicated statistical significance ($p < 0.05$) for both stiffness and tension increases at pCa 6.1. The increase in stiffness indicates that MgADP increased the number of strongly bound cross-bridges at submaximal Ca^{2+}. MgADP also increased the ratio of tension to stiffness by 23% at pCa 6.1, similar to the 19% increase observed at pCa 4.5.

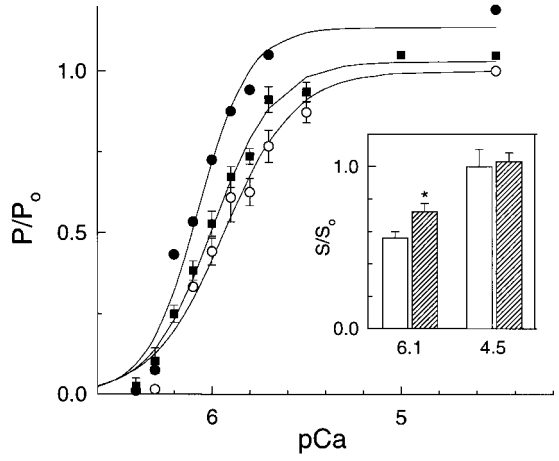

FIGURE 1 Effects of MgADP on steady-state tension and stiffness. Tension-pCa relationships in the absence (○) and presence of 0.5 mM MgADP (■) and 5 mM MgADP (●). Solid lines show fits to the Hill equation with $pCa_{50} = 5.98$, $n_H = 4.9$ (no ADP); $pCa_{50} = 6.08$, $n_H = 5.3$ (0.5 mM MgADP); and $pCa_{50} = 6.16$, $n_H = 6.3$ (5 mM MgADP). Using method 2 for statistical analyses (see Materials and Methods), these values were $pCa_{50} = 6.01 \pm 0.09$, $n_H = 4.8 \pm 0.8$ (no MgADP); $pCa_{50} = 6.09 \pm 0.08$, $n_H = 4.9 \pm 0.7$ (0.5 mM MgADP); and $pCa_{50} = 6.18 \pm 0.06$ (*), $n_H = 6.1 \pm 0.4$ (*). For double Hill plots (see Materials and Methods) values were $pCa_{50} = 6.0$, $n_{H1} = 3.7$, $n_{H2} = 1.6$ (no ADP); $pCa_{50} = 6.1$, $n_{H1} = 4.8$, $n_{H2} = 1.7$ (0.5 mM MgADP); and $pCa_{50} = 6.2$, $n_{H1} = 7.8$, $n_{H2} = 2.0$ (5 mM MgADP). (*Inset*) Effects of MgADP on sarcomere stiffness at pCa 4.5 and 6.1. Open bars are with no added MgADP, and hatched bars are in the presence of 5 mM MgADP. Stiffness was obtained by measuring changes in force and sarcomere length resulting from a 3.3-kHz sinusoidal length oscillation (see Materials and Methods). *$p <$ 0.05 compared with no MgADP. Error bars represent mean ± SEM from five to seven fibers.

Caged ADP tension transients

Illustrated in Fig. 2 *A* are representative tension transients resulting from photorelease of 0.5 mM MgADP within a skinned psoas fiber. Before photolysis, active tension was allowed to develop to a steady level. The fiber and surrounding solution were irradiated with a 1-ms flash of near-UV light to release ADP. Free Mg^{2+} in photolysis solutions was adjusted so that MgADP increased by 0.5 mM (see Materials and Methods). At full activation, isometric tension increased by 5% P_o (where P_o is the tension at pCa 4.5 without MgADP). Tension rose with an approximately exponential time course and an observed rate constant, k_{ADP}, of 9.7 s^{-1} (Fig. 2 *A*, *trace b*). The new tension level was maintained for 2 s, after which the fiber was released by 10% of its length, allowed to shorten for 15 ms, and then re-extended to its original length. This protocol permitted comparative measurements of the caged ADP tension transient and the rate constant of tension re-development, k_{tr}, under similar conditions (Fig. 2 *A*). A MgADP-induced tension transient with a larger amplitude and slower kinetics was observed in the same fiber at submaximal levels of activator Ca^{2+} ($P/P_o = 0.5$; Fig. 2 *A*, *trace c*, and see below).

To confirm that the changes in tension after photolysis were the expected magnitude, we compared the amplitude of the caged ADP tension rise with the effects of MgADP on steady-state tension. At maximal Ca^{2+}, photorelease of 0.5 mM MgADP and addition of 0.5 mM MgADP increased tension by a similar amount (5% P_o vs. 4–5% P_o) (Fig. 1). At submaximal Ca^{2+}, steady-state tension increased by 5–20% P_o due to the presence of 0.5 mM MgADP, and photorelease of 0.5 mM MgADP resulted in tension increases in this same range (Fig. 3 *B*; see below). Overall, the

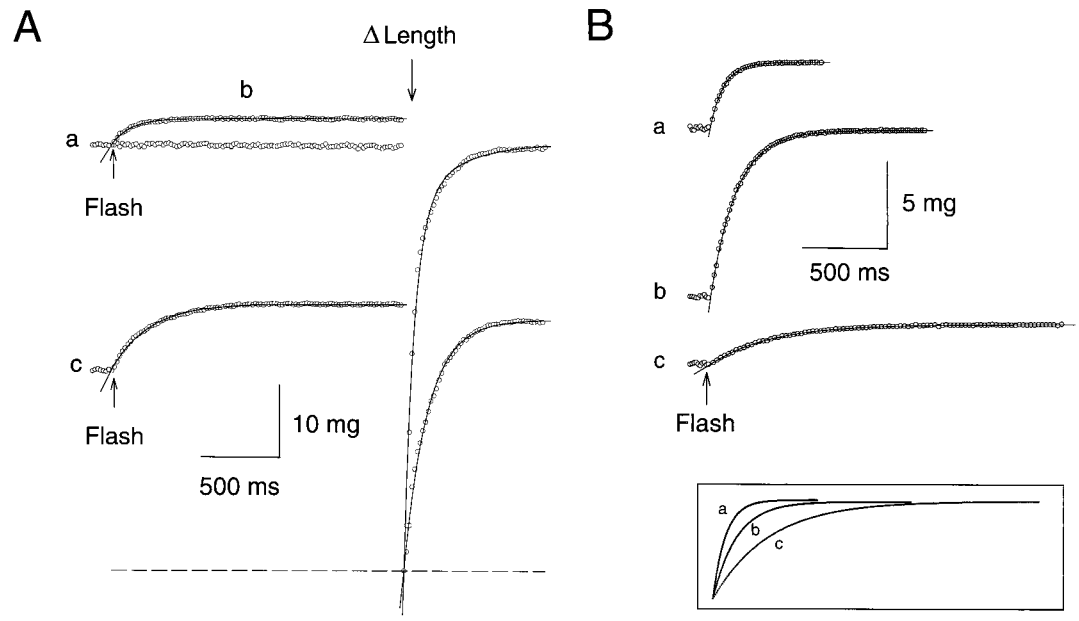

FIGURE 2 Representative traces showing the effects of Ca^{2+} concentration on the caged ADP tension transient. (*A*) Pulse irradiation of a fiber at pCa 4.5 in the absence of caged ADP (*a*), at pCa 4.5 in the presence of 5.2 mM caged ADP (*b*), or at pCa 5.8 in the presence of 5.2 mM caged ADP (*c*). The photo-released MgADP concentration was 0.5 mM. After tension achieved a plateau, the fiber was released by 10% of its length, allowed to shorten for 15 ms, and then re-stretched to its original length for measurement of k_{tr}. Rate constants obtained from single-exponential fits were as follows: (*a*) k_{tr} = 11.8 s^{-1}; (*b*) k_{ADP} = 10.1 s^{-1}, k_{tr} = 11.5 s^{-1}; (*c*) k_{ADP} = 5.3 s^{-1}, k_{tr} = 6.6 s^{-1}. The dotted line represents the level of zero force for all three records. (*B*) Caged ADP transients at three different pCa levels all in the same fiber: (*a*) pCa 4.5; (*b*) pCa 5.9; (*c*) pCa 6.4. Tension levels before and after photolysis were: 1.0–1.05 P_o at pCa 4.5; 0.44–0.63 P_o at pCa 5.9; and 0.0–0.05 P_o at pCa 6.4. (*Inset*) Amplitudes were normalized and fit to single exponentials (——). Apparent rate constants, k_{ADP}, were as follows: (*a*) 10 s^{-1} at pCa 4.5; (*b*) 4.2 s^{-1} at pCa 5.9; and (*c*) 1.6 s^{-1} at pCa 6.4.

effects of MgADP on tension were similar in steady-state and photorelease experiments.

Ca^{2+} sensitivity of the caged ADP tension transient

Fig. 2 *B* shows several representative caged ADP tension transients at different pCa values. Solid lines show that the data are well fit by single exponentials. In the inset, the exponential fits are normalized in amplitude and plotted on the same time base to illustrate differences in rates. The data clearly show that under conditions of submaximal Ca^{2+} activation, caged ADP tension transients are slower than those recorded during maximal activation. Summarized in Fig. 3 *A* are the effects of Ca^{2+} on k_{ADP} as well as a comparison between k_{ADP} and the rate of tension re-development, k_{tr}, determined sequentially in the same fiber. When measured at 0.5 mM MgADP, k_{ADP} increased five-fold as pCa was reduced from 6.5 to 4.5 (i.e., [Ca^{2+}] was increased). It is clear from Fig. 3 *A* that k_{ADP} was similar to k_{tr} in both rate and sensitivity to Ca^{2+}.

The amplitude of the caged ADP tension transient changed with variations in pCa in a relatively complicated manner. This is summarized in Fig. 3 *B*. The relationship was bell-shaped, increasing steeply to a peak of 22% P_o at pCa of ~6.1, then declining to a residual value of 5% near full activation. At pCa values between 6.5 and 6.3, active tension was close to zero (<5% P_o) before photolysis so that after photolysis tension development was almost exclusively the result of the sudden increase in MgADP (for example, see Fig. 2 *B*, *trace c*). Between pCa 6.3 and 5.7, significant active tension had developed before photogeneration of MgADP. And yet, amplitudes of the caged ADP transients were largest in this range (Fig. 3 *B*; original records in Fig. 2 *B*). These caged ADP measurements revealed a three- to fourfold potentiation of MgADP-induced tension rises at intermediate Ca^{2+} levels. Between pCa 5.8 and 4.5 pre-flash active tension approached its maximum (>70% P_o), and the amplitude of the transient was constant at ~5% P_o.

Effects on transients due to variations in P_i and MgADP concentration

Previous characterization of the caged ADP tension transient at full Ca^{2+} activation showed that the rate of the transient slowed as MgADP concentration was elevated, but became faster as P_i concentration was elevated, providing insight into the underlying mechanisms of MgADP effects (Lu et al., 1993). Here we compared the effects of variations in MgADP and P_i concentration at high and low Ca^{2+}. The presence of 10 mM P_i in the photolysis solution influenced

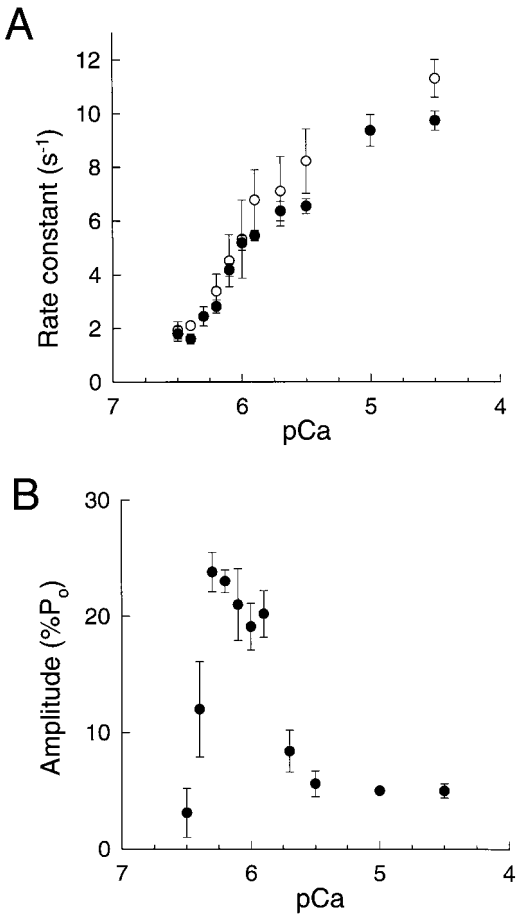

FIGURE 3 Summary of effects of Ca^{2+} on k_{tr} and the rate and amplitude of caged ADP tension transients. (*A*) k_{ADP} (●) and k_{tr} (○) versus pCa measured sequentially in the same fibers following photorelease of 0.5 mM MgADP. (*B*) Amplitude of the caged ADP transient normalized to maximum tension in the absence of MgADP and plotted versus pCa. Data represent mean ± SEM for eight fibers.

the caged ADP transient similarly at high and low Ca^{2+}. The transient became biphasic, requiring a double-exponential fit (Fig. 4 *A*); also, 10 mM P_i increased the rate of the fast phase by about threefold at both high and low Ca^{2+} (Fig. 4 *B*). Moreover, the Ca^{2+} sensitivity of the transient was largely unchanged by the presence of P_i (Fig. 4 *B*).

To establish the dependence on MgADP concentration at low Ca^{2+}, we compared the effects of photorelease of 0.1 mM MgADP (no added MgADP) with photorelease of 0.5 mM MgADP in the presence of 3.5 mM MgADP. Isometric tension before photolysis was equalized in the two cases by adjusting the pCa of the activating solution. The net result of this protocol was that final MgADP concentration was either 0.1 mM or 4 mM, but initial tension values and transient amplitudes were similar at the two MgADP concentrations (not shown). We observed that the caged ADP transient was slower by 10–20% at the higher MgADP concentration over the entire range of Ca^{2+} activation (not shown). This and the earlier experimental results with P_i indicate that the kinetic pathways being probed by photorelease of MgADP have the same properties as those examined previously at high Ca^{2+} (Lu et al., 1993).

Effects of NEM-S1 on caged ADP tension transients

Preincubation of fibers with 4 μM NEM-S1 had little effect on maximal tension but significantly altered the tension-pCa relationship (Fig. 5 *A*), consistent with earlier results (Swartz and Moss, 1992). NEM-S1 treatment mainly increased isometric tension at pCa $>$ pCa_{50}, resulting in a significant reduction of the steepness of the steady-state tension-pCa relationship (Fig. 5 *A*). The Hill coefficient decreased from 7.8 ± 1.2 to 5.0 ± 0.8 ($p < 0.05$), but the change in pCa_{50} was not statistically significant (Fig. 5 *A*). Because a single Hill plot did not give an ideal fit to the data, a double Hill plot transformation was also used (Moss et al., 1983). The Hill coefficient for the steeper part of the relationship (i.e., pCa $>$ pCa_{50}) decreased by 2.5-fold due to NEM-S1 treatment, whereas the Hill coefficient for the shallower part (pCa $<$ pCa_{50}) decreased by just 1.5-fold (not shown). The results from both types of Hill analysis were consistent with NEM-S1 causing a significant reduction of the apparent cooperativity of Ca^{2+}-induced thin filament activation. When the difference in steady-state tension before and after NEM-S1 treatment was plotted versus pCa (Fig. 5 *A*, *inset*) the largest difference was observed at a pCa of ~6.1. This difference plot is strikingly similar to the caged ADP amplitude versus pCa plot (Fig. 3 *B*). This comparison supports the notion that potentiation of tension around pCa 6.1 by MgADP is due to effects of newly formed MgADP-bound cross-bridges on the level of thin filament activation, an effect that was mimicked by the addition of NEM-S1.

NEM-S1 treatment also had dramatic effects on the caged ADP tension transient, but only under conditions of submaximal Ca^{2+} activation. At full Ca^{2+} activation, NEM-S1 was without effect on the tension response to caged ADP. At pCa 6.1, NEM-S1 treatment increased k_{ADP} to its maximal rate (the rate observed at pCa 4.5) (Fig. 5 *B*). This effect of NEM-S1 was concentration dependent, with a half-maximal acceleration at ~2 μM and a complete effect at 6–10 μM NEM-S1 (Fig. 5 *B*, *inset*). This is similar to the NEM-S1 concentration range that increased steady-state tension and k_{tr} at submaximal Ca^{2+} in an earlier study (Swartz and Moss, 1992). In the present experiments, steady-state tension at pCa ~6.3 increased from 0.01 P_o to 0.1 P_o after treatment with 4 μM NEM-S1 (Fig. 5 *A*). The effects of NEM-S1 on k_{ADP} over a range of pCa values are summarized in Fig. 6 *A*. The fivefold change in k_{ADP} with variation in Ca^{2+} was essentially eliminated following a 20-min incubation of fibers with 8 μM NEM-S1. The rate was near maximal at all levels of Ca^{2+} activation (Fig. 6 *A*).

The amplitude of the caged ADP tension transient was also dramatically altered by NEM-S1 treatment. Potentia-

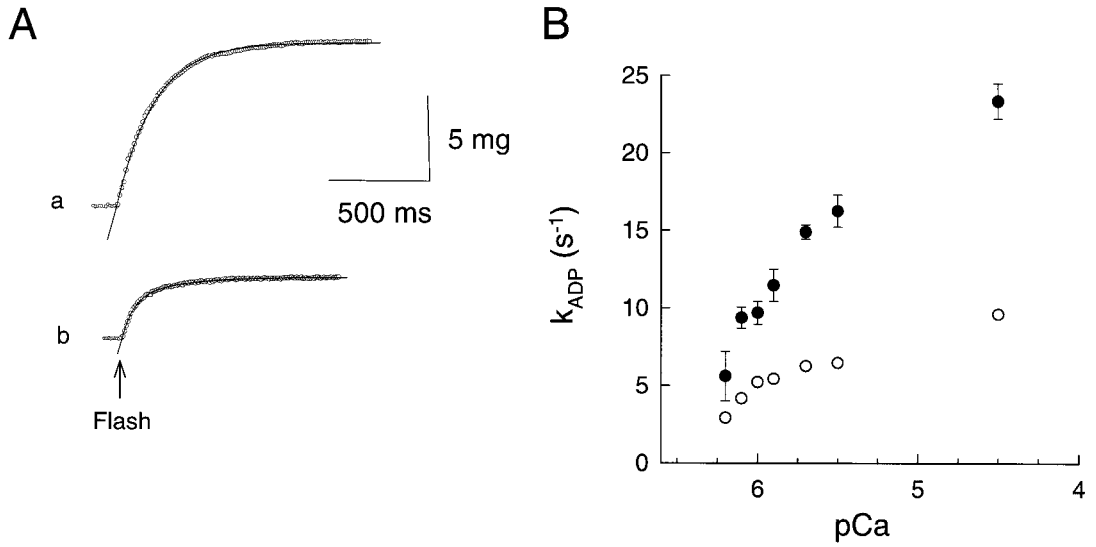

FIGURE 4 Effects of P_i on caged ADP tension transients at submaximal Ca^{2+}. (*A*) Original tension records at pCa 6.1, no added P_i (*a*), or at pCa 6.1, 10 mM P_i (*b*). Solid lines show fits to a single-exponential function with $k_{ADP} = 3.4\ s^{-1}$ (no P_i) (*a*) or to a double-exponential function with $k_{ADP} = 9.3\ s^{-1}$ (fast phase) and $k_{slow} = 0.9\ s^{-1}$ (slow phase) (*b*). Tension levels before and after photolysis were as follows: (*a*) 0.25–0.41 P_o; (*b*) 0.02–0.10 P_o. In the presence of P_i, the fast phase represented 61% of the amplitude of tension transient. (*B*) Ca^{2+} dependence of k_{ADP} (fast phase) at two different P_i concentrations: (○), no added P_i; (●), 10 mM P_i.

tion of the amplitude at intermediate Ca^{2+} was greatly reduced, leaving a residual amplitude of 4–7% P_o across most of the pCa range examined (Fig. 6 *B*). From these data it is apparent that there exists an NEM-S1-sensitive component to the amplitude (between ~5% and ~22% P_o at 0.5 mM MgADP) and an NEM-S1-insensitive component (between 0 and ~5% P_o at 0.5 mM MgADP). Thus, the caged ADP tension transient was still detectable after NEM-S1 treatment, but the large effects on rate and amplitude due to varying the level of Ca^{2+} activation were no longer observed. This finding further supports the idea that MgADP increases isometric tension at submaximal Ca^{2+} predominantly by influencing thin filament activation as a result of formation of MgADP-bound bridges. The presence of an NEM-S1-insensitive component of the caged ADP transient is consistent with the finding that MgADP also increases isometric tension by other means, i.e., by increasing the average force per cross-bridge. This NEM-S1-insensitive increase in force per cross-bridge was most noticeable at maximal levels of Ca^{2+} activation but was also apparent at submaximal Ca^{2+}.

DISCUSSION

This work is an extension of an earlier study in skinned skeletal muscle fibers in which the kinetics of the MgADP-induced tension increase were examined at a maximum level of Ca^{2+} activation (Lu et al., 1993). Here we report the influence of varying the level of activator Ca^{2+} or the number of bound cross-bridges on the response of skeletal fibers to MgADP.

MgADP effects on steady-state tension and stiffness

MgADP shifted the tension-pCa relationship to the left, indicating an increase in the apparent Ca^{2+} sensitivity of tension development. A similar effect of MgADP was reported in slow skeletal muscle fibers (Hoar et al., 1987). Cooperativity as determined by Hill coefficients increased modestly as MgADP concentration was raised, but given the inexact control of MgATP and MgADP levels within fibers during these measurements we want to be cautious about interpreting this small change. At maximal Ca^{2+}, the absence of an observable stiffness increase even though tension rose by nearly 20% demonstrates a clear change in mechanical properties of cross-bridges in the presence of MgADP (see also Dantzig et al., 1991; Seow and Ford, 1997). At submaximal Ca^{2+}, stiffness did increase in the presence of MgADP, suggesting that under these conditions MgADP increased the number of attached cross-bridges (Ford et al., 1977). It has been shown that the actin filament may contribute up to half of the sarcomere compliance of skinned fibers (Higuchi et al., 1995). This complicates interpretation of stiffness measurements because sarcomere stiffness is not linearly related to the number of attached cross-bridges. However, our steady-state stiffness and tension measurements show fairly clearly that MgADP influences sarcomere stiffness only at low Ca^{2+}. This suggests that only at submaximal Ca^{2+} levels does formation of MgADP-cross-bridge complexes activate thin filament sites either within the same regulatory unit or in a neighboring unit that results in additional cross-bridges entering states

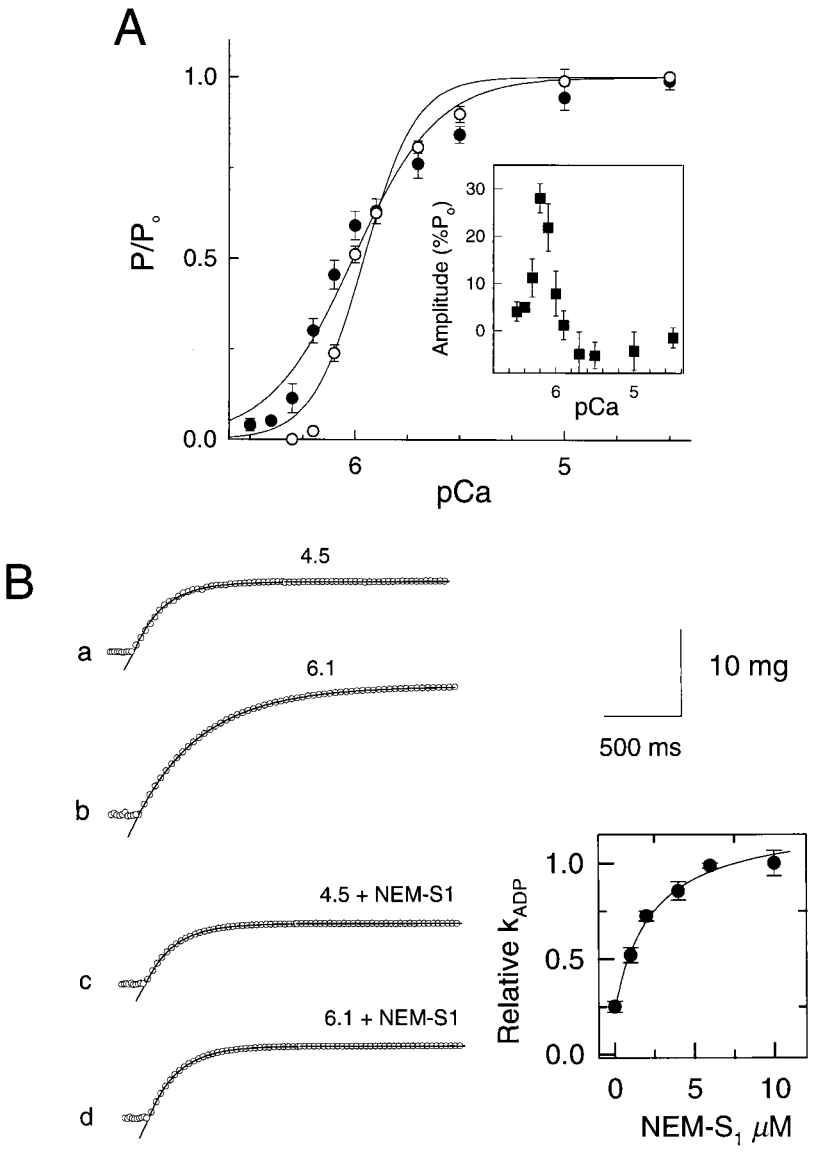

FIGURE 5 Effects of NEM-S1 on steady-state tension and kinetics. (*A*) Tension-pCa relationships before (○) and after (●) treatment with 4 μM NEM-S1. (*Inset*) Difference in steady-state tension with and without NEM-S1. Data are expressed as mean ± SEM from seven fibers, and error bars are shown when larger than symbols. Solid lines show fits to a Hill equation. Using method 2 for statistical analysis (see Materials and Methods), $pCa_{50} = 6.08 \pm 0.10$, $n_H = 7.8 \pm 1.2$ before and $pCa_{50} = 6.12 \pm 0.08$, $n_H = 5.0 \pm 0.8$ after NEM-S1. Only the change in n_H was statistically significant ($p < 0.05$). For a double Hill transformation (see Materials and Methods) values were $pCa_{50} = 6.0$, $n_{H1} = 8.5$, $n_{H2} = 1.8$ (no NEM-S1); $pCa_{50} = 6.1$, $n_{H1} = 3.4$, $n_{H2} = 1.1$ (NEM-S1). (*B*) Original records showing effects of NEM-S1 on caged ADP tension transients; 0.5 mM MgADP was released at the arrow and transients were fit to a single-exponential function (——). (*a*) pCa 4.5, no NEM-S1, $k_{ADP} = 11.2\ s^{-1}$; (*b*) pCa 6.1, no NEM-S1, $k_{ADP} = 3.2\ s^{-1}$; (*c*) pCa 4.5, after 8 μM NEM-S1, $k_{ADP} = 10.1\ s^{-1}$; (*d*) pCa 6.1, after 8 μM NEM-S1, $k_{ADP} = 9.4\ s^{-1}$. Tension levels before and after photolysis were as follows: (*a*) 1.0–1.05 P_o; (*b*) 0.22–0.36 P_o; (*c*) 1.0–1.05 P_o; (*d*) 0.40–0.46 P_o. (*Inset*) Dependence of k_{ADP} (normalized to its maximum) on NEM-S1 concentration at pCa 6.1. The solid line indicates a fit of the data to the equation: relative $k_{ADP} = ([\text{NEM-S1}]/(K_m + [\text{NEM-S1}])) + k_{ADP\text{-min}}$, with $K_m = 2\ \mu$M and $k_{ADP\text{-min}} = 0.23$. Data are from four fibers.

that contribute to tension and stiffness. This interpretation of the stiffness measurements is supported by the differential effects of NEM-S1 on caged ADP tension transients at maximal and submaximal Ca^{2+}. NEM-S1 reduces the effects of MgADP at submaximal Ca^{2+} presumably via its effects on the activation state of the thin filament. In contrast, tension transients at high Ca^{2+} were not influenced by NEM-S1, consistent with these tension increases being independent of thin filament activation state or cooperativity.

NEM-S1 effects on steady-state tension

The main effect of NEM-S1 on the tension-pCa relationship was observed at calcium levels below the midpoint of the steady-state tension-pCa curve. NEM-S1 increased force at pCa values $> pCa_{50}$ and also caused the Hill coefficient in this region, n_{H1}, to be reduced by 2.5-fold from 8.5 to 3.4. The Hill coefficient for the upper region of the curve was also reduced from 1.8 to 1.1, but we hesitate to place much significance on this finding because NEM-S1 has a modest inhibitory effect on tension development in this range of calcium (see also Swartz and Moss, 1992). The importance of the double Hill analysis is that it demonstrates clearly that the tension-pCa relationship is made up of at least two components. At very low levels of calcium (pCa > 6), NEM-S1 has large effects on steady-state tension, indicating that contributions to thin filament activation by bound cross-bridges is important in this region of the curve. At higher calcium levels (pCa < 5.8), NEM-S1 has much less effect on tension, thin filament activation and cooperativity. It is interesting to note that MgADP also influences tension development differently at high and low levels of calcium activation. Although this is not readily apparent from looking at the steady-state tension-pCa curves (Fig. 1), it is quite

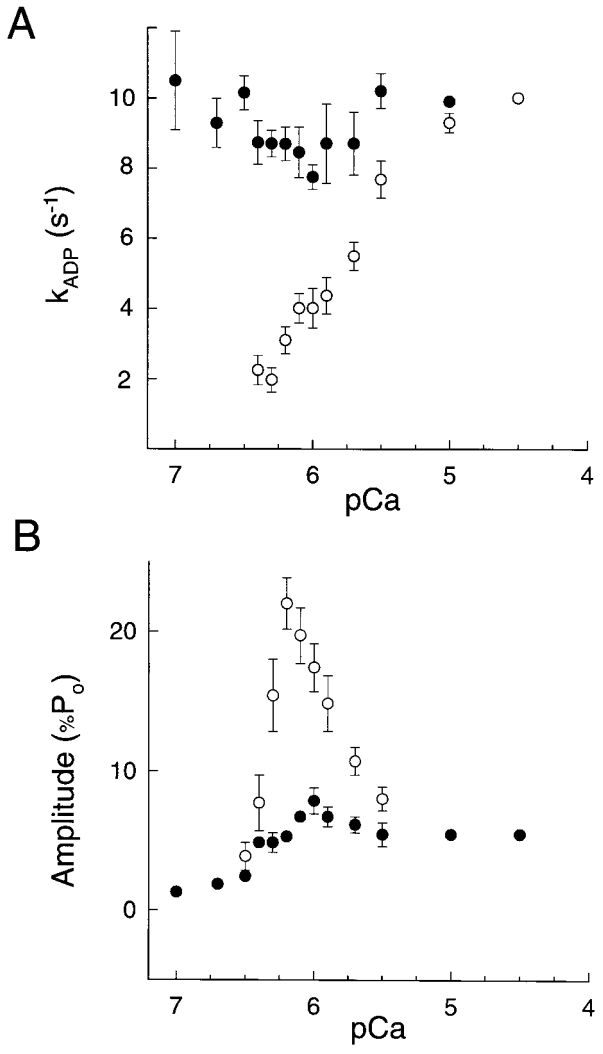

FIGURE 6 Summary of effects of NEM-S1 on Ca^{2+} dependence of caged ADP tension transients. (*A*) k_{ADP} versus pCa before (○) and after (●) treatment with 8 μM NEM-S1; (*B*) Amplitude of the caged ADP tension transient (relative to P_o) versus pCa before (○) and after (●) 8 μM NEM-S1. Mean ± SEM for seven fibers.

apparent from the amplitude of the caged ADP tension transients, which are potentiated at pCa $<$ 5.8 but relatively constant at pCa $>$ 5.8 (Fig. 3 *B*). Potentiation of tension development by MgADP is likely due to cross-bridge-mediated activation of the thin filament because it is largely abolished by treatment of fibers with NEM-S1 (Fig. 6 *B*).

Kinetic regulation via the thin filament

The caged ADP tension transient provides further evidence in support of the notion that kinetic transitions in the cross-bridge cycle are influenced by the level of Ca^{2+} activation (Brenner, 1988; Metzger et al., 1989; Swartz and Moss, 1992). The kinetics of the caged ADP tension transient were similar to the kinetics of tension redevelopment, k_{tr}, measured under the same conditions (Fig. 3). k_{tr} was also sensitive to Ca^{2+} to a similar degree (Fig. 3 *A*) (Brenner, 1988; Metzger and Moss, 1989). A potentially important difference in the measurements is that k_{ADP} does not involve special mechanical perturbations for cross-bridge detachment, which could lead to thin filament inactivation and the need for reactivation during tension development (Millar and Homsher, 1990). The similarities observed here between k_{ADP} and k_{tr} indicate that the rate of tension development is highly calcium dependent even when thin filament inactivation does not occur. Both kinetic processes do appear to be Ca^{2+} regulated via the thin filament regulatory system, because treatment of fibers with NEM-S1 greatly reduced the dependence of both on Ca^{2+} concentration (Fig. 6 *A*) (Swartz and Moss, 1992). NEM-S1 is thought to function by binding with high affinity to actin sites and influencing endogenous cross-bridges indirectly by switching the thin filament into a more fully activated state.

The properties of caged ADP transients were not only similar to k_{tr} transients, they were also similar to the tension development process initiated by photolysis of caged Ca^{2+} (Araujo and Walker, 1994, 1996). The rate of each of these tension development processes increased 5–15-fold over the physiological range of Ca^{2+}, and each was accelerated by inclusion of P_i in the medium. Using rapid mixing with individual skeletal myofibrils to minimize diffusional delays, Tesi et al. (2000) recently found that MgADP jumps increased force with a similar time course to k_{tr}, although they did not explore the dependence of this tension rise on calcium or P_i. Interestingly, rapid reductions in the P_i concentration also increased force with kinetics virtually identical to k_{tr}, including large dependencies on Ca^{2+} and P_i concentrations (Tesi et al., 2000).

The graded nature of the tension-pCa relationship could be a reflection of gradual switching of functional units from a fully off conformation to a fully on conformation (Brandt et al., 1987), or it could be due to functional units existing in partially activated states (Moss et al., 1985). The finding that tension development rates measured by caged ADP photolysis varied in a graded rather than an all-or-none manner with Ca^{2+} concentration is more compatible with the existence of partially activated states. Reduced rates of tension development appear to be one manifestation of a partially activated thin filament. Moreover, this partially activated condition exists in the steady state and does not require mechanical maneuvers such as those used to initiate a k_{tr} transient (i.e., a period of shortening followed by a re-extension) (Brenner, 1988).

It is presently unclear which step in the cross-bridge cycle might be subject to regulation by Ca^{2+} through the thin filament regulatory system. Two characteristics of the tension rise were a decrease in rate with elevated MgADP concentration and an acceleration of the rate with elevated P_i. These observations suggest a mechanism for the tension rise that involves slowing of cross-bridge detachment re-

sulting from inhibition of MgATP binding by MgADP and a net increase in cross-bridge flux through early steps in the cycle including P_i release (Lu et al., 1993). The effects of increasing MgADP and P_i were similar at submaximal and maximal Ca^{2+}, suggesting that the same kinetic pathways predominate regardless of the Ca^{2+} level.

Dual regulation of the cross-bridge cycle

Although NEM-S1 accelerated k_{ADP} to near its maximum when Ca^{2+} was submaximal, it was able to increase steady-state tension only from 0.01 P_o to ~0.1 P_o (at a pCa of ~6.3). The differential effects of NEM-S1 on isometric tension and kinetics of tension development suggest the possibility that the thin filament regulates muscle contraction by not only kinetically regulating the distribution of cross-bridges between weakly and strongly bound states (Brenner, 1988; Metzger and Moss, 1989) but also by regulating recruitment of cross-bridges into the cycle (Dantzig et al., 1988), i.e., a dual regulation by the thin filament as suggested by McKillop and Geeves (1993) and by Campbell (1997). These differential effects could have other explanations. For example, NEM-S1 may artifactually prevent maximal tension development by occupying most of the available actin sites. However, even in the presence of 8 μM NEM-S1, fibers could generate more than 80% of maximal tension at pCa 4.5 (Fig. 5*A*) (Swartz and Moss, 1992). Another possibility is that NEM-S1 may not be uniformly distributed within the fibers, such that rates are dominated by localized NEM-S1 effects but overall tension increases only slightly. Several lines of evidence indicate that NEM-S1 is fairly uniformly distributed. First, the time course of the caged ADP tension transients are well described by single exponentials at all activation levels, which is not compatible with the existence of two populations of cross-bridges cycling at significantly different rates. Second, NEM-S1 treatment essentially eliminated the large MgADP-induced potentiation of isometric tension at submaximal Ca^{2+}. Because caged ADP itself is likely to equilibrate uniformly within the fiber interior, the large reduction of its potentiating effects by NEM-S1 argues for similar distributions of caged ADP and NEM-S1. Finally, confocal imaging of a fluorescent NEM-S1 was consistent with nearly uniform distribution in fibers (Swartz and Moss, 1992). The differential effects on kinetics and isometric tension are probably manifestations of dual regulation of the cross-bridge cycle via the thin filament. Several features of the data including the Ca^{2+} dependence of rates and amplitudes of the caged ADP tension transient can be accounted for by a simple model similar to that of Campbell (1997). This model is presented in an Appendix and Fig. 7.

CONCLUSIONS

The rate and Ca^{2+} dependence of force development initiated by a MgADP-jump was similar to the widely studied k_{tr} transient. The rate of the MgADP-induced tension transient increased by fivefold over the physiological range of Ca^{2+}, and the amplitude was potentiated at intermediate levels of Ca^{2+}. Treatment of fibers with NEM-S1, which cooperatively activates the thin filament regulatory system, eliminated these effects of submaximal Ca^{2+} on the rate and amplitude of the tension transient. In contrast, NEM-S1 had no discernable effect on the response to MgADP at high Ca^{2+}. We conclude that MgADP promoted force development in skinned psoas fibers in two ways, both of which involve MgADP binding to nucleotide-free cross-bridges. First, MgADP increased the apparent force per cross-bridge, which was most readily detected at high Ca^{2+}. Second, MgADP promoted thin filament activation at submaximal Ca^{2+}. Overall, the data provide evidence that cooperative interactions between cross-bridges and the Ca^{2+} regulatory system play a major role in the apparent kinetic regulation of the cross-bridge cycle by Ca^{2+}.

APPENDIX

A model of regulation

The results presented here can be summarized in a simple model of thin filament regulation of the cross-bridge cycle (Fig. 7 *A*). In this model, cross-bridges can exist in one weakly attached state (W) or three strongly attached states (F, force generating; R, rigor; R-ADP, rigor with ADP bound). The cross-bridge can also be in a detached state although this state is not shown in Fig. 7. F represents the force-generating state, and so the W-to-F step (step 1) is the force-generating kinetic transition defined by rate constants k_1 and k_{-1}. F is converted slowly and irreversibly to a rigor-like state (R-ADP) in step 2 before the dissociation of MgADP. Dissociation of MgADP (step 3) gives the rigor state (R). R can react with MgADP to return to R-ADP or with MgATP to return to the weakly attached state (W) via step 4. Ca^{2+} regulation of the cross-bridge cycle is assumed to occur as follows. Detached cross-bridges enter the cycle initially as weakly attached bridges by a traditional steric blocking type of mechanism. Once recruited, the cross-bridge can interconvert between the four states in Fig. 7 *A*. The W-to-F transition is also assumed to be controlled by Ca^{2+} and by the number of cross-bridges in the R-ADP state. This is accomplished by making the forward rate constant k_1 a function of the concentrations of Ca^{2+} and R-ADP (as defined in the Fig. 7 legend). This model is consistent with the model of Campbell (1997) and of McKillop and Geeves (1993), which features three states of the thin filament with a blocked-to-closed transition controlled by Ca^{2+} and a closed-to-open isomerization controlled by strong S1 binding.

Figs. 7, *B* and *C*, shows that this dual regulation model accounts for several of the features of the caged ADP tension transients at submaximal Ca^{2+}. It provides an explanation for the response to caged ADP photolysis itself. The rapid elevation of MgADP causes a rapid shift of R to R-ADP, which increases the value of k_1 and in turn shifts more W cross-bridges to F. It also provides an explanation for why cooperative activation of the thin filament by cross-bridges does not lead to an explosive all-or-none activation of tension development. If some limit is not introduced into the system, the regenerative (i.e., positive feedback) nature of the process would continue until k_1 reached its maximum value and steady-state force reached its maximum. Dual regulation of the type described here limits the number of cross-bridges recruited into the cycle at any given Ca^{2+}, thereby limiting the extent to which force can develop. Another aspect of the model that contributes to a simple exponential time course is the feature that only R-ADP cross-bridges influence the kinetic transition, as these represent a minor component of the total cross-bridge population. The influence of nucleotide-free rigor bridges is assumed to be insignificant due to their brief lifetime resulting in a vanishingly small popu-

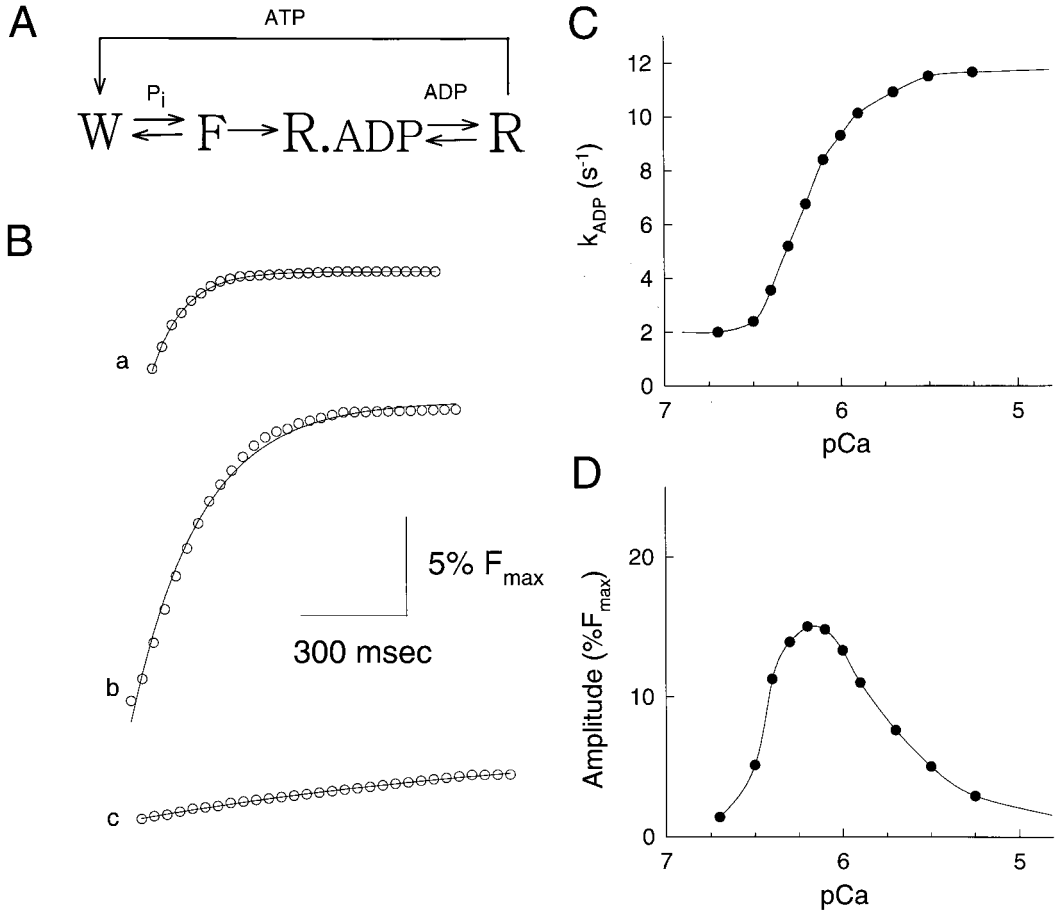

FIGURE 7 Model of regulation of the cross-bridge cycle by Ca^{2+} and by cross-bridges. (*A*) Four-state kinetic model: W, weak binding state; F, force-generating state; R-ADP, rigor with ADP bound; R, rigor. Simulations of the model were performed by numerical integration of four differential equations: $W'(t) = k_{-1}[P_i][F] + k_4[ATP][R] - k_1[W]$; $F'(t) = k_1[W] - k_{-1}[P_i][F] - k_2[F]$; $R\text{-}ADP'(t) = k_2[F] + k_{-3}[R][ADP] - k_3[R\text{-}ADP]$; $R'(t) = k_3[R\text{-}ADP] - k_4[ATP][R] - k_{-3}[ADP][R]$; with $W = [Ca]^n/([Ca]^n + K_{Ca}{}^n)$ at time = 0 and $k_1 = k_{1max}(([Ca]^n/([Ca]^n + K_{Ca}{}^n) + (1 - ([Ca]^n/([Ca]^n + K_{Ca}{}^n))([R\text{-}ADP]^n/([R\text{-}ADP]^n + K_{R\text{-}ADP}{}^n)))$. Values for constants were: $k_{1max} = 8\ s^{-1}$, $k_{-1} = 1$, $k_2 = 2$, $k_3 = 25\ s^{-1}$, $k_{-3} = k_4 = 10^6\ M^{-1}\ s^{-1}$, $n = 2$, $K_{Ca} = 10^{-6}$ M, $K_{R\text{-}ADP} = 0.001$, and [ATP] = 5 mM. (*B*) Simulations of caged ADP tension transients at 0.3 μM Ca^{2+} (pCa 6.5) (*a*), 0.8 μM Ca^{2+} (pCa 6.1) (*b*), and 2 μM Ca^{2+} (pCa 5.7) (*c*). To simulate caged ADP transients, the distribution of states at a given Ca^{2+} was permitted to reach a steady state at 0.05 mM ADP. Then ADP was changed to 0.5 mM and the resulting increase in force ([F] + [R-ADP] + [R]) is shown. Lines illustrate fits to single exponentials. (*C*) Rate constant of simulated traces versus pCa. (*D*) Amplitude of simulated traces normalized to maximum force at high Ca^{2+} (F_{max}).

lation under steady-state conditions. Consistent with this assumption, rigor-ADP cross-bridges have been shown to cooperatively activate the thin filament much more effectively than nucleotide-free rigor bridges (Thirlwell et al., 1994). In the model, tension rises at a rate determined by k_1, which depends upon both MgADP concentration and Ca^{2+}. Thus, the model also explains the apparent Ca^{2+} dependence of k_{ADP} (Fig. 7 *C*). P_i accelerates the simulated rate of tension development by increasing the $k_{-1}[P_i]$ term in the model. The bell-shaped amplitude of the caged ADP tension transients versus pCa is qualitatively reproduced (Fig. 7 *D*).

In the context of the model, addition of NEM-S1 is equivalent to introducing R-ADP bridges into the system independent of Ca^{2+} and MgADP. The predicted effect is an increase of k_1 to its maximum, and thus the rate of the W to F transition to its maximum as observed (Fig. 6 *A*). The presence of an excess of R-ADP bridges would also be expected to eliminate the effects of changes in R-ADP on k_1 (the second term in the equation of the Fig. 7 legend), thereby eliminating potentiation of the amplitude. Further refinements of this model will be needed to explain all of the results, such as the effect of MgADP on apparent force per cross-bridge, and the precise mechanism of the tension increase at high Ca^{2+} (Dantzig et al., 1991; Lu et al., 1993). The simple model of Fig. 7 does reproduce a number of basic features of the caged ADP tension transients at submaximal Ca^{2+}, including its approximate exponential time course, the dependence of rate on pCa, and the bell-shaped dependence of amplitude on pCa.

This work was supported by National Institutes of Health grants HL44114 to J.W.W. and HL25861 to R.L.M.

REFERENCES

Araujo, A., and J. W. Walker. 1994. Kinetics of tension development in skinned cardiac myocytes initiated by photorelease of Ca^{2+}. *Am. J. Physiol.* 267:H1643–H1653.

Araujo, A., and J. W. Walker. 1996. Phosphate release and force generation in cardiac myocytes investigated by photolysis of caged phosphate and caged calcium. *Biophys. J.* 70:2316–2326.

Ashley, C. C., I. P. Mulligan, and T. J. Lea. 1991. Ca^{2+} and activation mechanisms in skeletal muscle. *Q. Rev. Biophys.* 24:1–73.

Brandt, P. W., M. S. Diamond, and J. J. Rutchik. 1987. Co-operative interactions between troponin-tropomyosin units extend the length of the thin filament in skeletal muscle. *J. Mol. Biol.* 195:885–896.

Brandt, P. W., D. Roemer, and F. H. Schachat. 1990. Co-operative activation of skeletal muscle thin filaments by rigor cross-bridges. *J. Mol. Biol.* 212:437–480.

Bremel, B., and A. Weber. 1972. Cooperation within actin filaments in vertebrate skeletal muscle. *Nat. New Biol.* 238:97–101.

Brenner, E. 1988. Effect of Ca^{2+} on cross-bridge turnover kinetics in skinned single rabbit psoas fibers: implication for regulation muscle contraction. *Proc. Natl. Acad. Sci. U.S.A.* 85:3265–3269.

Campbell, K. 1997. Rate constant of muscle force redevelopment reflects cooperative activation as well as cross-bridge kinetics. *Biophys. J.* 72: 254–262.

Chalovich, J. M., P. B. Chock, and E. Eisenberg. 1981. Mechanism of action of troponin-tropomyosin. *J. Biol. Chem.* 256:575–578.

Chalovich, J. M., and E. Eisenberg. 1982. Inhibition of actomyosin ATPase activity by troponin without blocking binding of myosin to actin. *J. Biol. Chem.* 257:2432–2437.

Dantzig, J. A., M. G. Hibberd, D. R. Trentham, and Y. E. Goldman. 1991. Cross-bridge kinetics in the presence of MgADP investigated by photolysis of caged ATP in rabbit psoas muscle fibers. *J. Physiol.* 432: 639–680.

Dantzig, J. A., J. W. Walker, D. R. Trentham, and Y. E. Goldman. 1988. Relaxation of muscle fibers with adenosine 5′[γthio]triphosphate (ATP[γS]): evidence for Ca^{2+} dependent affinity of rapidly detaching zero-force cross-bridges. *Proc. Natl. Acad. Sci. U.S.A.* 85:6716–6720.

Fabiato, A. 1988. Computer programs for calculating total from specified free or free from specified total ionic concentration in aqueous solutions containing multiple metals and ligands. *Methods Enzymol.* 157: 378–417.

Ford, L. E., A. F. Huxley, and R. M. Simmons. 1977. Tension responses to sudden length change in stimulated frog muscle fibers near slack length. *J. Physiol.* 269:441–515.

Glantz, S. A., and B. K. Slinker. 1990. Primer of Applied Regression and Analysis of Variance. McGraw Hill, New York.

Gordon, A. E., E. Homsher, and M. Regnier. 2000. Regulation of contraction in striated muscle. *Physiol. Rev.* 80:853–924.

Greene, L. E., and E. Eisenberg. 1980. Cooperative binding of myosin subfragment-1 to the actin-troponin-tropomyosin complex. *Proc. Natl. Acad. Sci. U.S.A.* 77:2616–2620.

Haselgrove, J. C. 1973. X-ray evidence for a conformational change in the actin-containing filaments of vertebrate striated muscle. *Cold Spring Harbor Symp. Quant. Biol.* 37:341–352.

Higuchi, H., T. Yanagida, and Y. E. Goldman. 1995. Compliance of thin filaments in skinned fibers of rabbit psoas muscle. *Biophys. J.* 69: 1000–1010.

Hoar, P. E., C. W. Mahoeny, and W. G. L. Kerrick. 1987. MgADP increases maximum tension and Ca^{2+} sensitivity in skinned rabbit soleus fibers. *Pflug. Arch.* 10:30–36.

Huxley, H. E. 1973. Structural changes in actin- and myosin-containing filaments during contraction. *Cold Spring Harbor Symp. Quant. Biol.* 37:361–376.

Lu, Z., R. L. Moss, and J. W. Walker. 1993. Tension transients initiated by photogeneration of MgADP in skinned skeletal muscle fibers. *J. Gen. Physiol.* 101:867–888.

McKillop, D. F. A., and M. A. Geeves. 1993. Regulation of the interaction between actin and myosin subfragment 1: evidence for three states of the thin filament. *Biophys. J.* 65:693–701.

Metzger, J. M., M. L. Greaser, and R. L. Moss. 1989. Variation in cross-bridge attachment rate and tension with phosphorylation of myosin in mammalian skinned skeletal muscle fibers. *J. Gen. Physiol.* 93: 855–883.

Millar, N. C., and E. Homsher. 1990. The effect of phosphate and calcium on force generation in glycerinated rabbit skeletal muscle fibers. *J. Biol. Chem.* 265:20234–20240.

Moss, R. L. 1999. Plasticity in the dynamics of myocardial contraction: calcium, crossbridge kinetics or molecular cooperation. *Circ. Res.* 84: 862–865.

Moss, R. L., G. G. Guilian, and M. L. Greaser. 1985. The effects of partial extraction of TnC upon tension development in skinned skeletal muscle fibers. *J. Gen. Physiol.* 86:585–600.

Moss, R. L., A. E. Swinford, and M. L. Greaser. 1983. Alterations of the Ca^{2+} sensitivity of tension development by single muscle at stretched lengths. *Biophys. J.* 43:115–119.

Nagashima, H., and S. Asakura. 1982. Studies on co-operative properties of tropomyosin-actin and tropomyosin-troponin-actin complex by the use of *N*-ethylmaleimide treated and untreated species of myosin subfragment 1. *J. Mol. Biol.* 155:409–428.

Parry, D. A. D., and J. M. Squire. 1973. Structural role of tropomyosin in muscle regulation: analysis of the x-ray diffraction patterns from relaxed and contracting muscle. *J. Mol. Biol.* 75:33–55.

Rosenfeld, S. R., and E. Taylor. 1987. The mechanism of regulation of actomyosin subfragment 1 ATPase. *J. Biol. Chem.* 259:9984–9993.

Seow, C. Y., and L. E. Ford. 1997. Exchange of ATP for ADP on high force cross-bridges of skinned rabbit muscle fibers. *Biophys. J.* 72: 2719–2735.

Swartz, D. R., M. L. Greaser, and R. L. Moss. 1990. Regulation of binding of subfragment 1 in isolated rigor myofibrils. *J. Cell Biol.* 111: 2989–3001.

Swartz, D. R., and R. L. Moss. 1992. Influence of a strong binding myosin analog on calcium sensitive mechanical properties of skinned skeletal muscle fibers. *J. Biol. Chem.* 267:20497–20506.

Swartz, D. R., R. L. Moss, and M. L. Greaser. 1996. Calcium alone does not fully activate the thin filament for S1 binding to rigor myofibrils. *Biophys. J.* 71:1891–1904.

Tesi, C., F. Colomo, S. Nencini, N. Piroddi, and C. Poggesi. 2000. The effect of inorganic phosphate on force generation in single myofibrils from rabbit skeletal muscle. *Biophys. J.* 78:3081–3092.

Thirlwell, H., J. E. T. Corrie, G. P. Reid, D. R. Trentham, and M. A. Ferenczi. 1994. Kinetics of relaxation from rigor of permeabilized fast-twitch skeletal fibers from the rabbit using a novel caged ATP and apyrase. *Biophys. J.* 67:2346–2447.

Walker, J. W., Z. Lu, and R. L. Moss. 1992. Effects of Ca^{2+} on the kinetics of phosphate release in skeletal muscle. *J. Biol. Chem.* 267:2459–2466.

Walker, J. W., G. P. Reid, J. A. McCray, and D. R. Trentham. 1988. Photolabile 1-(2-nitrophenyl)ethyl phosphate esters of adenine nucleotide analogues. Synthesis and mechanism of photolysis. *J. Am. Chem. Soc.* 110:7170–7177.

White, D. C. S. 1970. Rigor contraction and the effect of various phosphate compounds on glycerinated insect flight and vertebrate muscle. *J. Physiol.* 208:583–605.

Williams, D. L., L. E. Greene, and E. Eisenberg. 1988. Cooperative turning on myosin subfragment 1 adenosine triphosphatase activity by the troponin-tropomyosin-actin complex. *Biochemisry.* 27:6987–6993.